Small-Scale Variability in MODIS and Pathfinder Sea Surface Temperatures With Applications to Data Error Models for in Situ Observations

[Poster materials for MODIS Science Team Meeting, University of Maryland University College, October 31, 2006; minor revisions: November 8, 2006]

Alexey Kaplan and Mark A. Cane
Lamont–Doherty Earth Observatory (LDEO) of Columbia University

Summary

SST is arguably the most visible climate variable in the public forum of climate change debate. In climate change detection and attribution studies they are usually used in the form of gridded data sets which are analyzed statistically or serve as boundary conditions for atmospheric general circulation models. Therefore it is of primary importance to ensure their optimality and reliability, especially for the pre-satellite data period, including reliability of their error estimates.

Most current methods of gridding blend together satellite and in situ data and involve a mixture of optimal interpolation (successive corrections), eigenvector reconstruction, bias correction techniques, and some forms of data assimilation [*Reynolds and Smith*, 1994; *Rayner et al.*, 2003; *Kaplan et al.*, 1997,2003]. Analyses of the pre-satellite period depend on quite sparse in situ data as their inputs, but they usually try to make use of statistical information extracted from the satellite period [*Smith et al.*, 1996,1998; *Rayner et al.*, 2003; *Kaplan et al.*, 2003]. Therefore, the quality of these analyses and hence our ability to detect and properly attribute long-term climate change hinges on the quality of a priori statistical information obtained from the satellite data.

The goal of this project is to make use of the extensive satellite data in order to quantify and model in situ data errors, and thus to improve pre-satellite era climate analyses. To this end we present intercomparisons of MODIS SST products, and their comparisons with Pathfinder V5 SST and the in situ data collection ICOADS. Further, we estimate small-scale and short-term variability of SST using satellite data sets. We then successfully use these estimates to model the magnitude of the the error in the binned in situ SST values.

Results

We present spatial patterns of total root-mean-square (RMS) difference and its separation into mean bias and the error standard deviation (STD) for many pairs of SST products. Figure 1 emphasizes the closeness of MODIS Terra SST and SST4 and presents the difference in the mean diurnal range captured by MODIS Terra observations vs Pathfinder SST. Variability estimates become significantly smaller if monthly averaging is applied (Figure 2). Apart from the year 2000, time variability of zonal means shows high temporal homogeneity (Figure 3). Figures 4 and 5 compare MODIS Terra SST with Pathfinder SST directly. We found the former to be slightly cooler than the latter, particularly in the midlatitudes.

We further performed the comparison of MODIS and Pathfinder temperature products with monthly $1^o \times 1^o$ summaries of in situ SSTs from ICOADS [*Woodruff et al.*, 1987; *Worley et al.*, 2005], a rather complete collection of historical ship and buoy surface observations (Figure 6). The comparison covered 2000-2005 period and found in situ measurements to be on average warmer than both night and day SST products. This is surprising, because ICOADS summaries here were not separated into day and time values and could be expected to fall in between day and night satellite SST products (differences we obtained are generally larger than the mean bulk-skin SST difference of $\sim 0.18^o$C [*Minnett*, 2003]. Per work of R.Evans and P.Minnett on the MODIS Science Team, the errors of MODIS SST products are only 0.3-0.4^{o}C, i.e. significantly smaller than most values of the STD of the SST difference shown in the right panels of Figure 6. Therefore, it is predominantly the error of the in situ data that we see here, and it needs to be investigated and modeled further. Statistics of the satellite to in situ data comparison computed for Pathfinder SST (Figure 7) is very similar to that computed for MODIS (Figure 6).

Figure 8 shows a seasonal cycle and meridional structure in zonally averaged temperature differences. It also shows a larger error of the Terra products (especially SST4) in the beginning of the record, during the year 2000. Comparisons of ICOADS with Pathfinder SSTs (Version 5) shows a similar magnitude of zonally averaged differences to those of MODIS (Figure 9).

We use 4 km Pathfinder satellite SST fields in order to estimate various components of the variability inside ICOADS $1^o \times 1^o$ monthly bins, and compute the total intra-bin variability estimate (Figure 10). Using these estimates σ, we attempt to model error in ICOADS as

$$e = \sigma / \sqrt{n_{\rm obs}},$$

where $n_{\rm obs}$ are numbers of individual ICOADS observations inside monthly $1^o \times 1^o$ bins. We then average calculated values of e with square over the period of Terra data products and compare the averaged error estimates with MODIS–ICOADS SST STD difference patterns (any of left-hand patterns in Figure 6).

The results indicate that in situ measurement errors must be taken into account. As Figure 11 shows, the standard deviations of ICOADS data inside their $1^o \times 1^o$ monthly bin are quite large, larger than space-time variability in these bins estimated from satellite data (Figure 10). With much sparser sampling of the ICOADS data, this is only possible if they are dominated by measurement error. These estimates are also consistent with the pattern of measurement error in ICOADS data calculated by *Kent and Challenor* [2006] using the variogram method (Figure 11). Adding the *Kent and Challenor* [2006] random error estimate to the physical variability estimates for 1^o bins significantly increases our estimate of the effective error in a single in situ observation (Figure 12). As Figure 13 demonstrates, the resulting error model, that assumes independence of individual in situ observations captures major spatial features of MODIS–ICOADS STD difference.

A similar effort for 5^o bins (Figures 14 and 15) also resulted in a realistic pattern, albeit of a smaller range. A plausible explanation of error underestimation (smaller range) is in effective non-independence of individual in situ measurements for 5^o bins, due to the the observations being concentrated along specific ship tracks and not randomly sampling 5^o bins.

Acknowledgements

This research was supported by the NASA grant NNG04GL28G "Small-scale variability in sea surface temperatures and climate analyses error." Discussions with Peter Minnett and Ken Casey are gratefully acknowledged, as well as the help from Ed Armstrong with data access. More information and data sets of the satellite SST and their variability statistics directly accessible via the Ingrid-based Data Catalog for easy data manipulation, visualization, and download in a variety of formats are available at
`http://rainbow.ldeo.columbia.edu/~alexeyk/Satellite_SST.html`.

References

Kaplan, A., Y. Kushnir, M. Cane, and M. Blumenthal, 1997: Reduced space optimal analysis for historical data sets: 136 years of Atlantic sea surface temperatures, *J. Geophys. Res.*, **102**, 27835–27860.

Kaplan, A., M. Cane, Y. Kushnir, A. Clement, M. Blumenthal, and B. Rajagopalan, 1998: Analyses of global sea surface temperature 1856-1991, *J. Geophys. Res.*, **103**, 18567-18589.

Kaplan A., M.A. Cane, and Y. Kushnir, 2003: Reduced space approach to the optimal analysis interpolation of historical marine observations: Accomplishments, difficulties, and prospects, in *Advances in the Applications of Marine Climatology: The Dynamic Part of the WMO Guide to the Applications of Marine Climatology*, WMO/TD-1081, World Meteorological Organization, Geneva, Switzerland, pp. 199-216.

Kent, E.C. and P. Challenor, 2006: Toward estimating climatic trends in SST. Part II: Systematic biases, *J. Atmos. Oceanic Technol.*, **23**, 476-486.

Minnett, P., 2003: Radiometric measurements of the sea-surface skin temperature: the competing roles of the diurnal thermocline and the cool skin, *Int. J. Remote Sensing*, **24**, 5033-5047.

Rayner, N.A., D.E.Parker, E.B.Horton, C.K.Folland, L.V.Alexander, D.P.Rowell, and A. Kaplan, 2003: Globally complete analyses of SST, sea ice, and night marine air temperature, 1871–2000, *J. Geophysical Res.*, **108**, 10.1029/2002JD002670.

Reynolds, R. W. and T. M. Smith, 1994: Improved global sea surface temperature analyses using optimum interpolation, *J. Climate*, **7**, 929-948.

Smith, T. M., R. W. Reynolds, R. E. Livezey, and D.C. Stokes, 1996: Reconstruction of historical sea surface temperatures using empirical orthogonal functions. *J. Climate*, **9**, 1403-1420.

Smith, T. M., R. E. Livezey, and S.S. Shen, 1998, An improved method for analyzing sparse and irregularly distributed SST data on a regular grid: The Tropical Pacific Ocean. *J. Climate*, **11**, 1717-1729.

Woodruff, S.D., R.J. Slutz, R.L. Jenne, and P.M. Steurer, 1987: A comprehensive ocean–atmosphere data set. *Bull. Amer. Meteor. Soc.*, **68**, 521-527.

Worley, S.J., S.D. Woodruff, R.W. Reynolds, S.J. Lubker, and N. Lott, 2005: ICOADS Release 2.1 data and products. *Int. J. Climatol.*, **25**, 823-842.

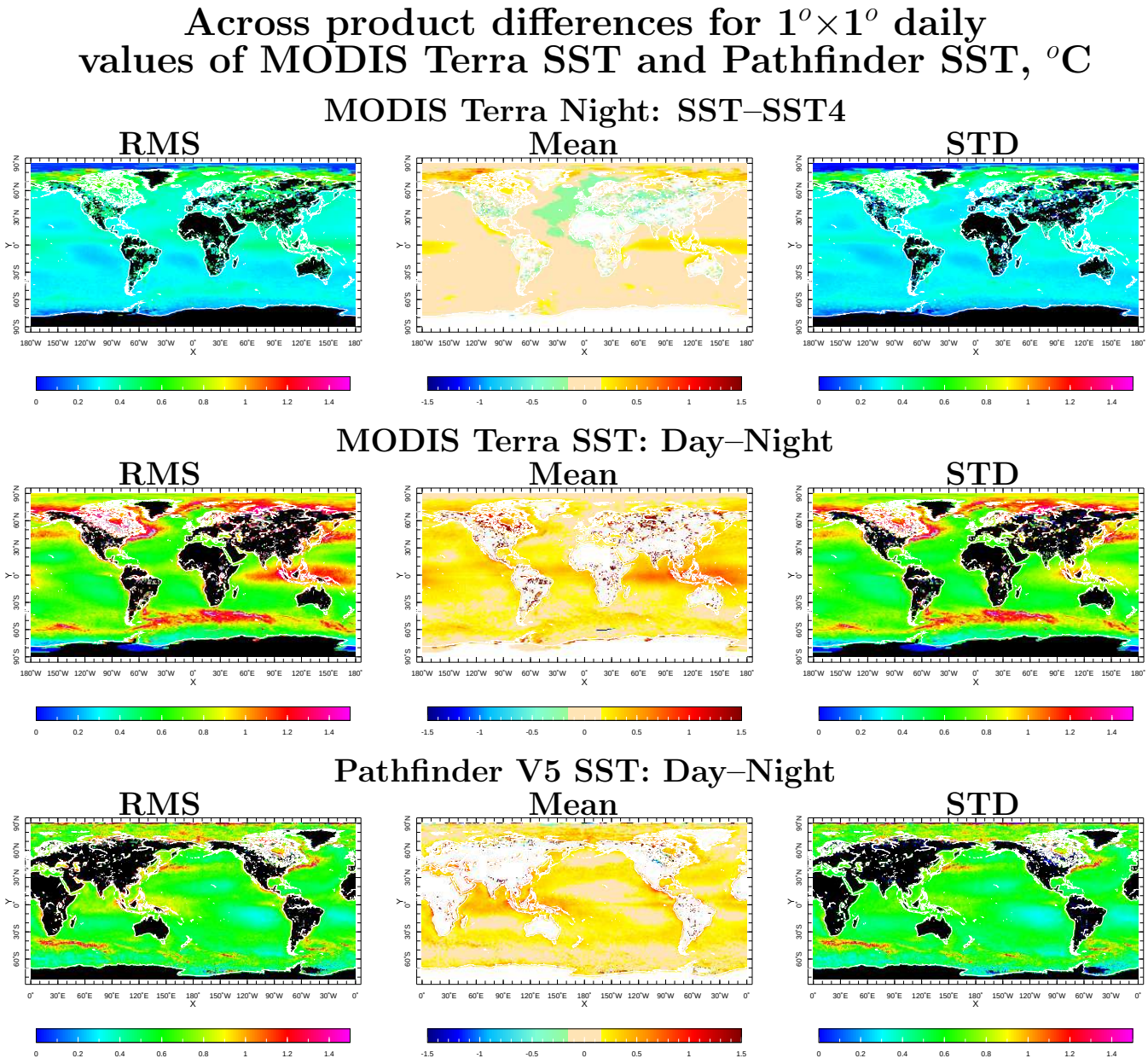

Figure 1: Across product differences for $1^o \times 1^o$ monthly values of MODIS Terra SST and Pathfinder SST. Left panels show RMS difference for 2000-2005 period, central and right panels subdivide it into the mean difference and standard deviations. Calculations performed for daily values. Units are ^{o}C.

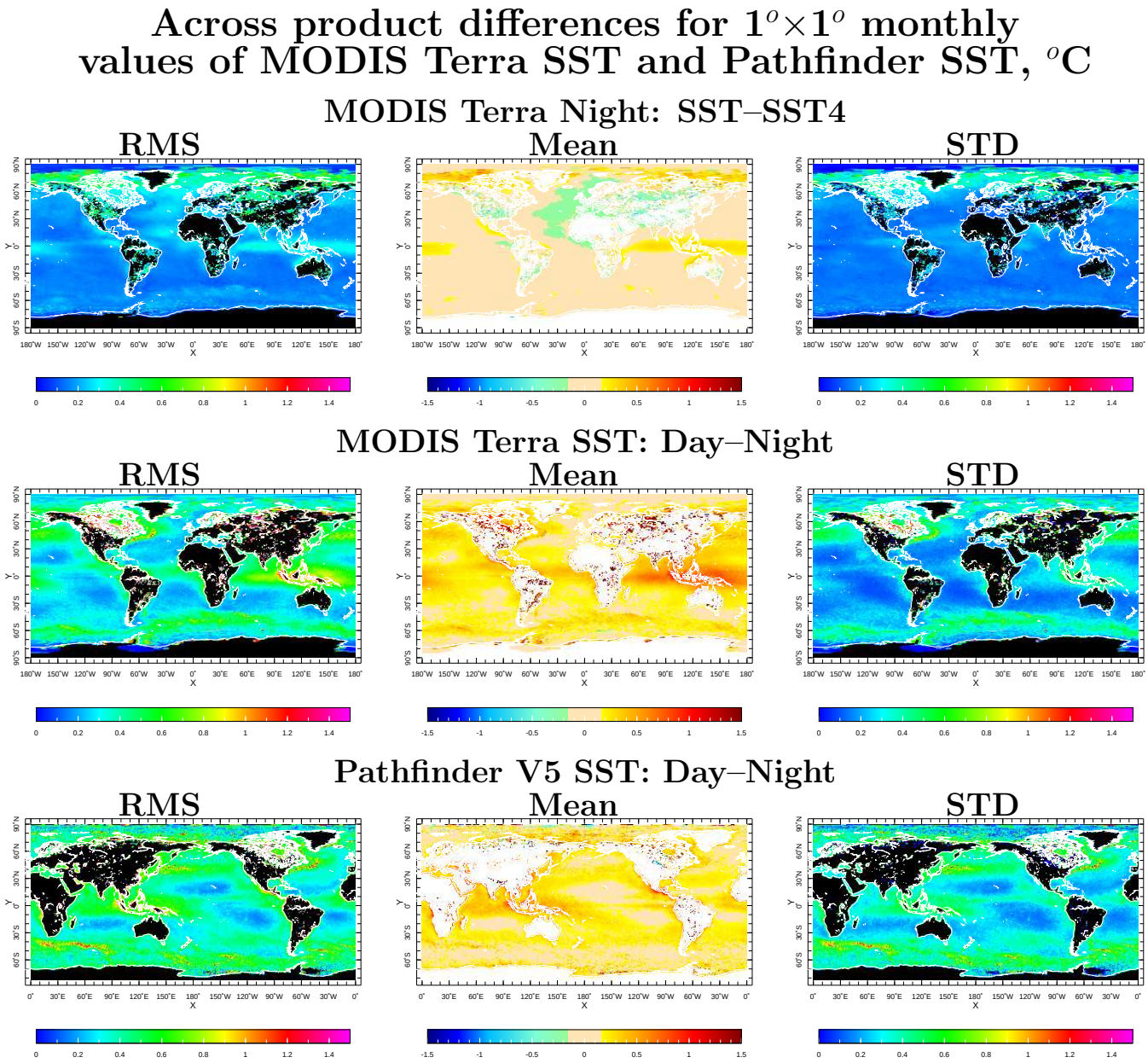

Figure 2: Across product differences for $1^o \times 1^o$ monthly values of MODIS Terra SST and Pathfinder SST. Left panels show RMS difference for 2000-2005 period, central and right panels subdivide it into the mean difference and standard deviations. Daily differences were averaged into monthly bins before calculating RMS, mean, and STD. Units are ^{o}C.

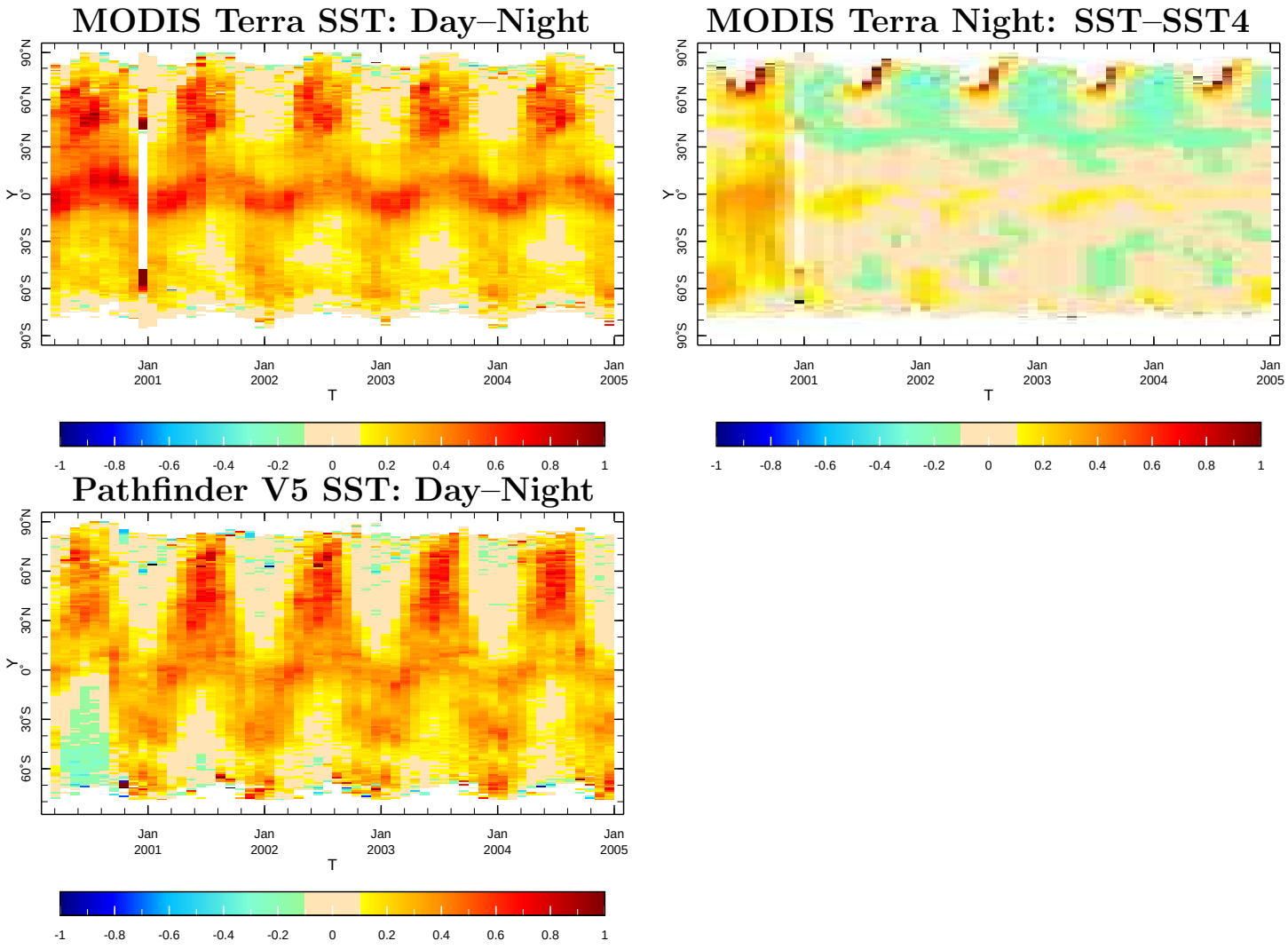

Figure 3: Zonal means of the monthly differences for SST products from MODIS Terra and Pathfinder V5. Units are ^{o}C.

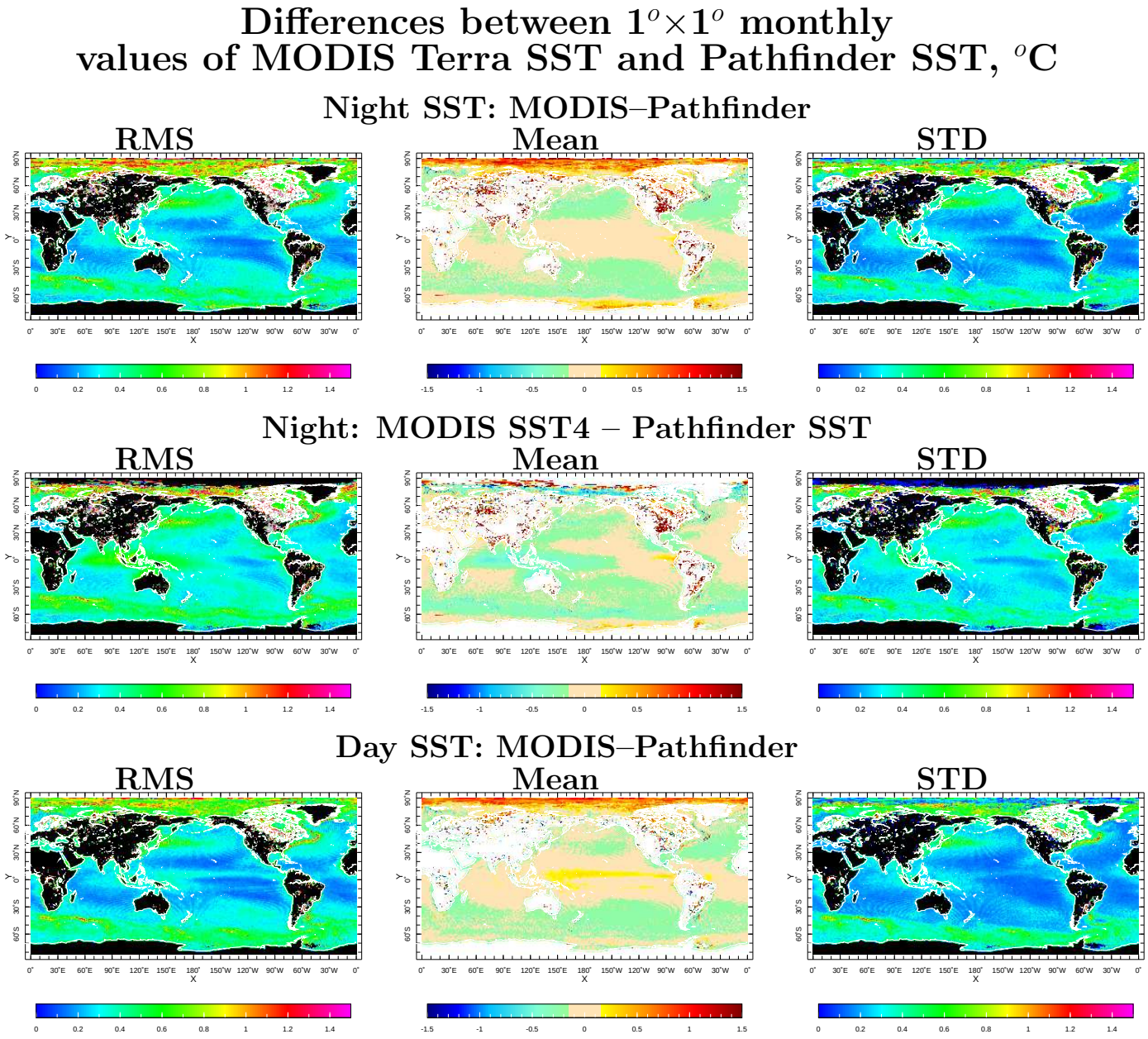

Figure 4: Differences between $1^o \times 1^o$ monthly values of MODIS Terra SST and Pathfinder SST. Left panels show RMS difference for 2000-2005 period, central and right panels subdivide it into the mean difference and standard deviations. Daily differences were averaged into monthly bins before calculating RMS, mean, and STD. Units are ^{o}C.

Across product zonal mean differences between $1^o \times 1^o$ monthly values of MODIS Terra SST and Pathfinder SST, ^{o}C

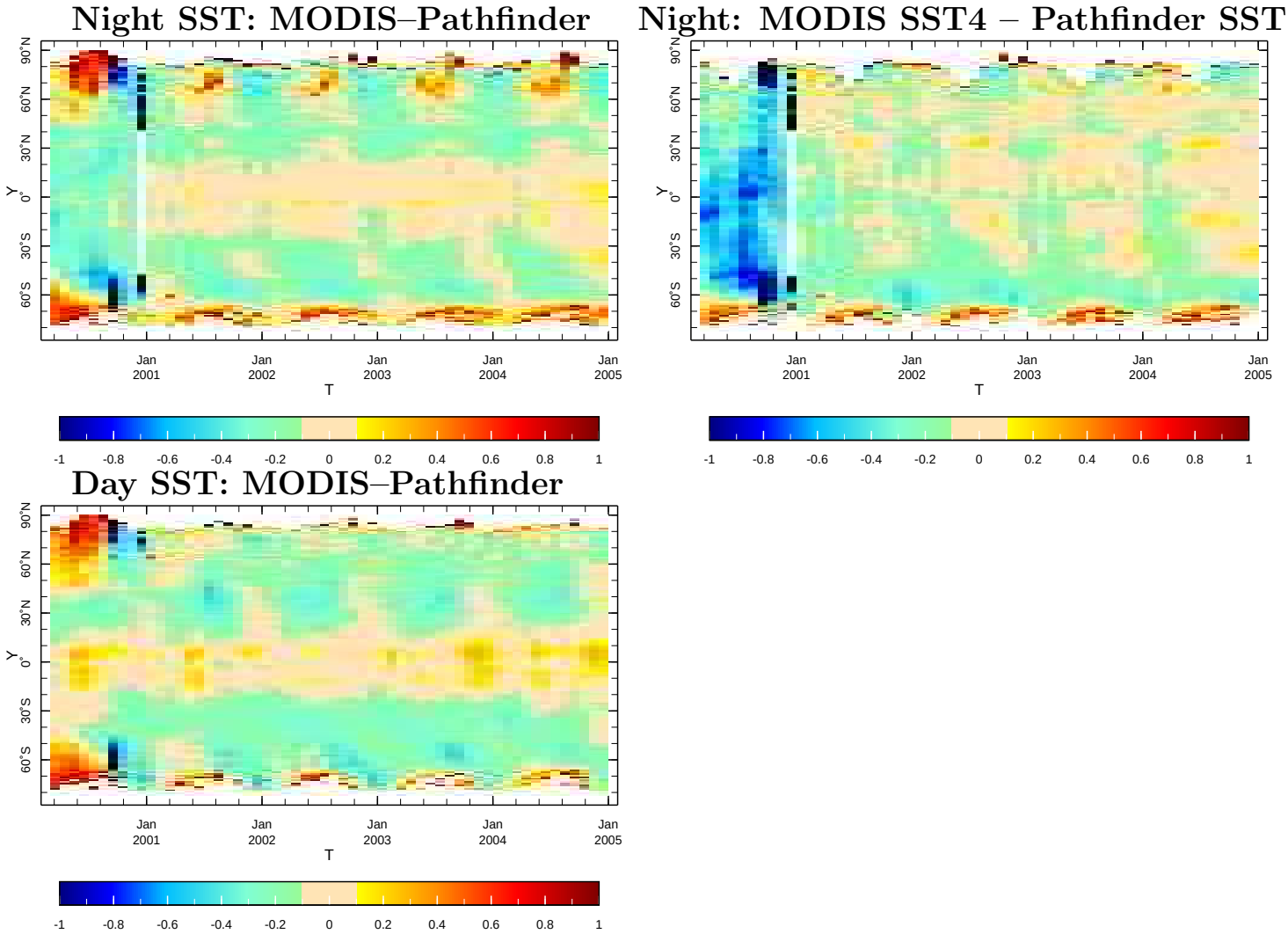

Figure 5: Zonal means of the monthly differences between SST products from MODIS Terra and Pathfinder V5. Units are ^{o}C.

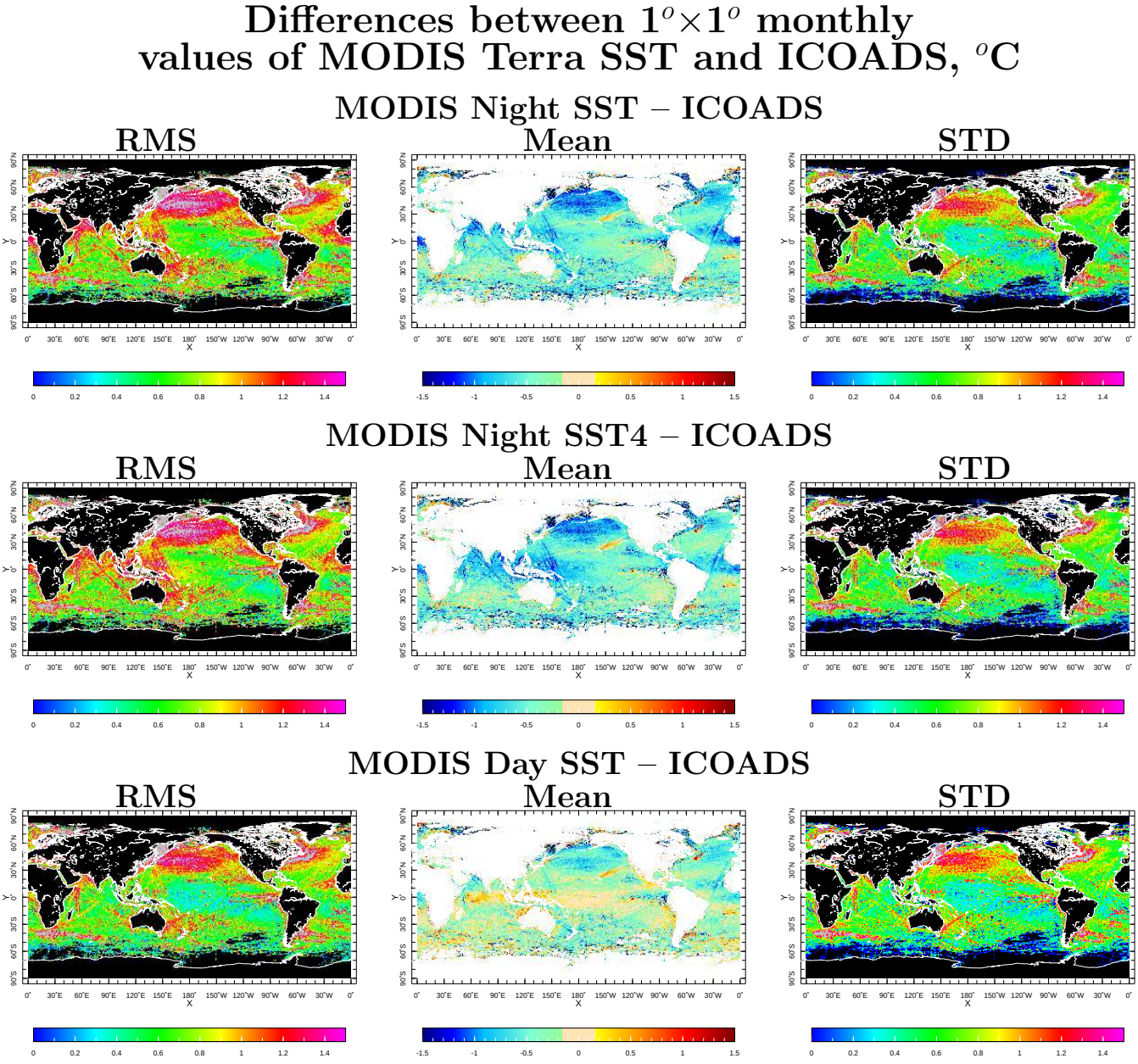

Figure 6: Difference between $1^o \times 1^o$ monthly summaries of MODIS SST values and ICOADS. Left panels show RMS difference for 2000-2005 period, central and right panels subdivide it into the mean difference and standard deviations. Daily differences were averaged into monthly bins before calculating RMS, mean, and STD. Units are ^{o}C. ICOADS observations were not separated for day and night.

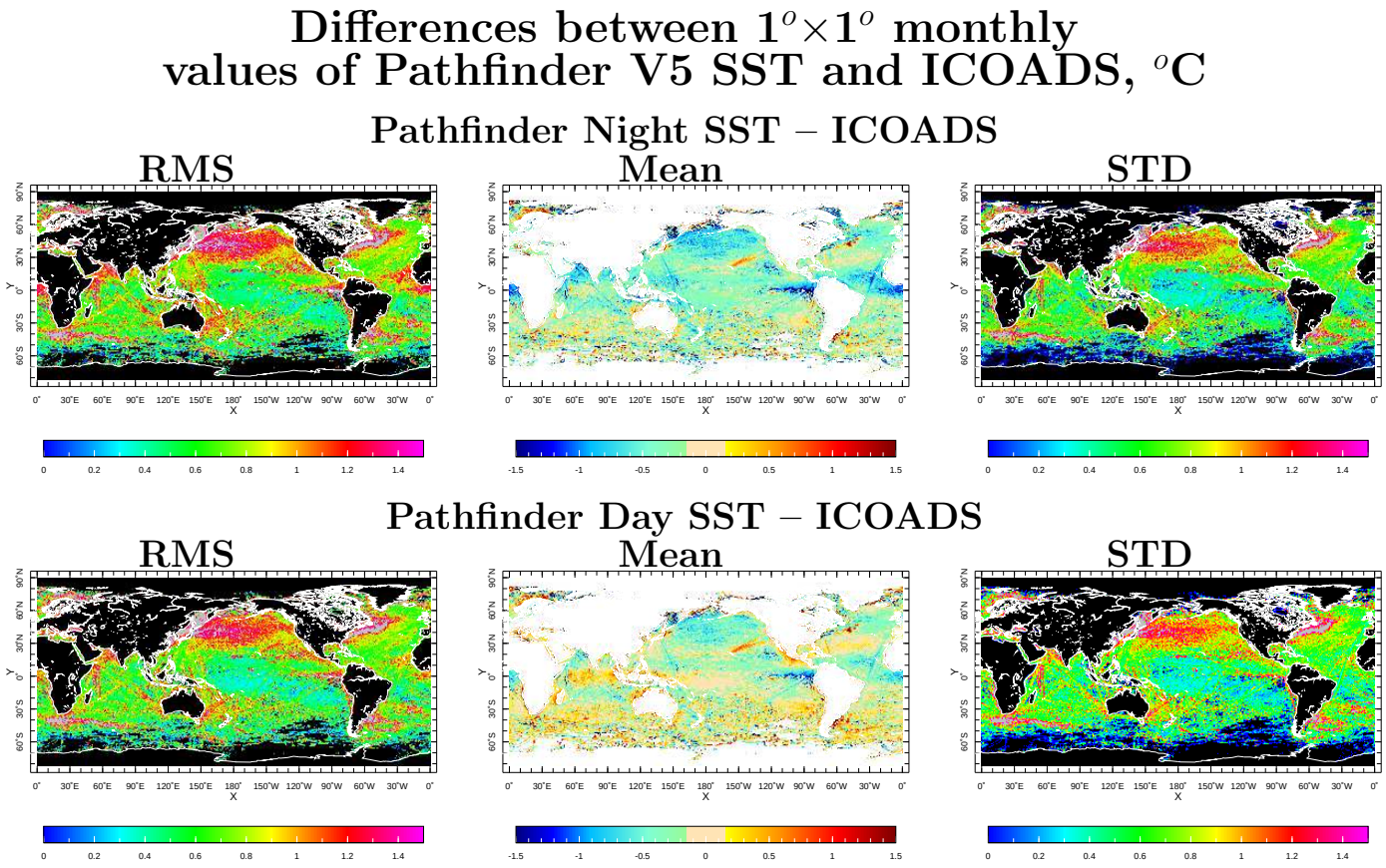

Figure 7: Difference between $1^o \times 1^o$ monthly summaries of Pathfinder V5 SST values and ICOADS. Left panels show RMS difference for 2000-2005 period, central and right panels subdivide it into the mean difference and standard deviations. Daily differences were averaged into monthly bins before calculating RMS, mean, and STD. Units are ^{o}C. ICOADS observations were not separated for day and night.

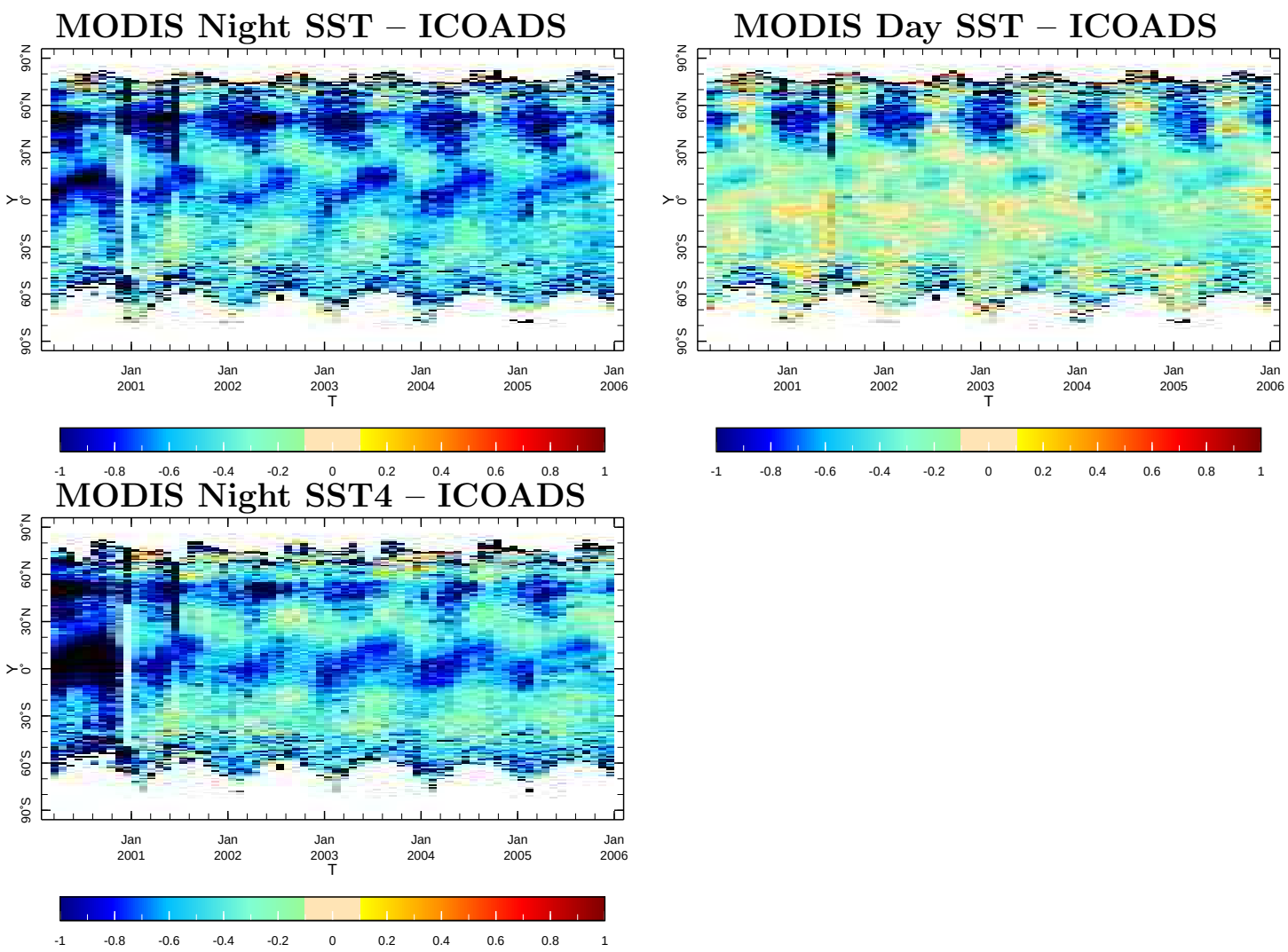

Figure 8: Zonal means of the difference between $1^o \times 1^o$ monthly summaries of Terra MODIS SST and ICOADS SST values. Top panels show the difference between MODIS and ICOADS SST products, the bottom panel is the same for the night SST4. Units are ^{o}C.

Zonal mean of the difference between $1^o \times 1^o$ monthly summaries of Pathfinder V5 SST and ICOADS, ^{o}C

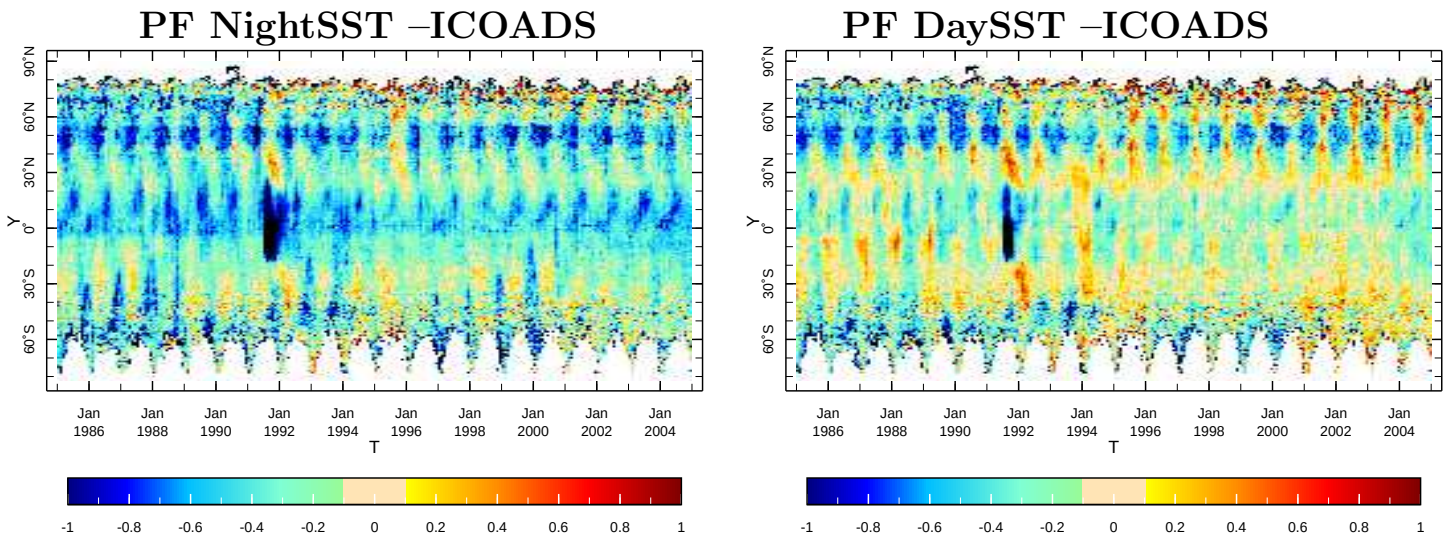

Figure 9: Same as Figure 8, but for Pathfinder V5 SST, instead of MODIS.

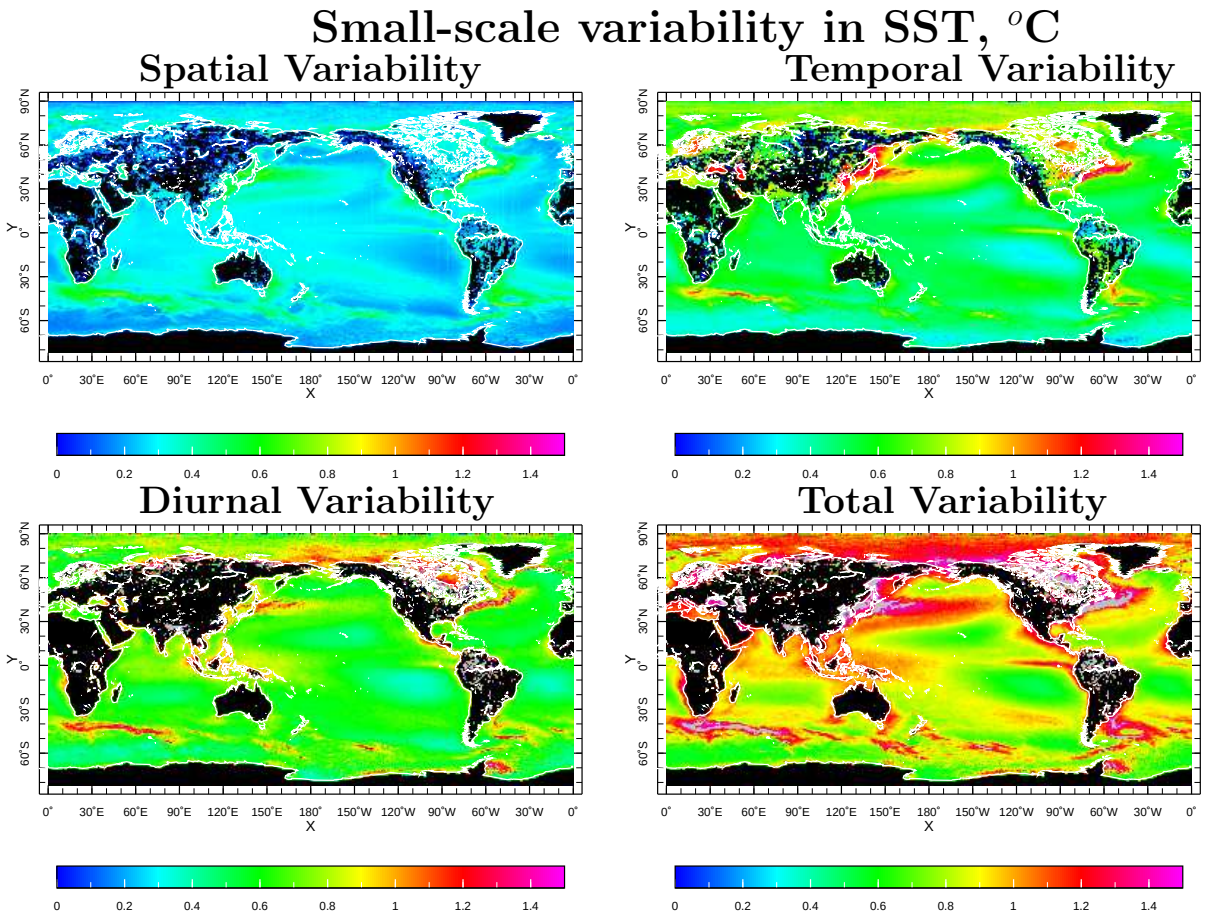

Figure 10: Estimates of standard deviation of SST variability, ^{o}C, estimated inside $1^o \times 1^o$ monthly bins.

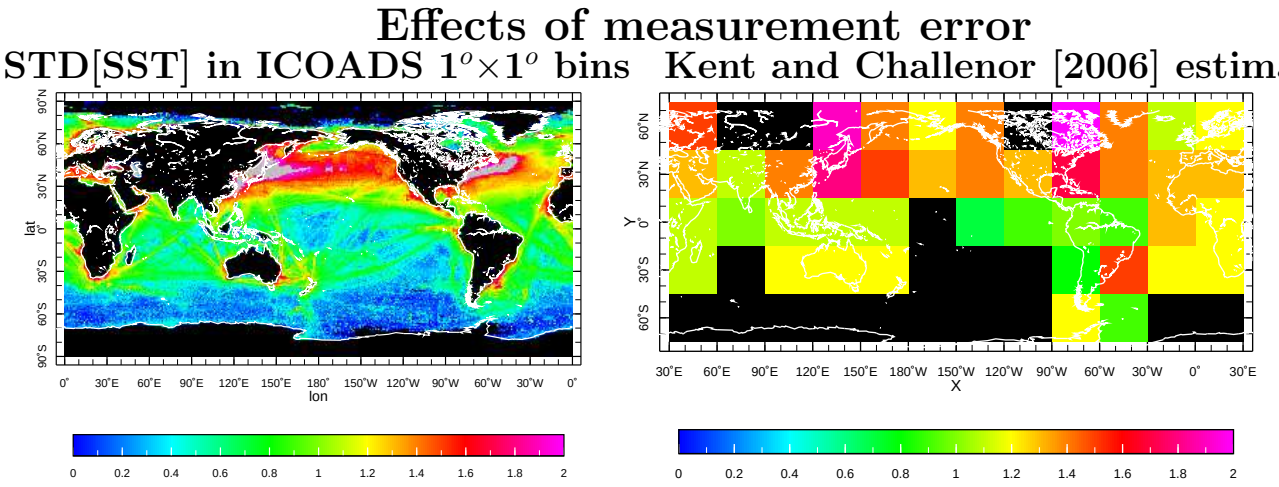

Figure 11: Effects of measurement error are seen in the field of standard deviations of SST measurements inside ICOADS $1^o \times 1^o$ monthly bins (left), and are estimated by the variogram method by *Kent and Challenor* [2006].

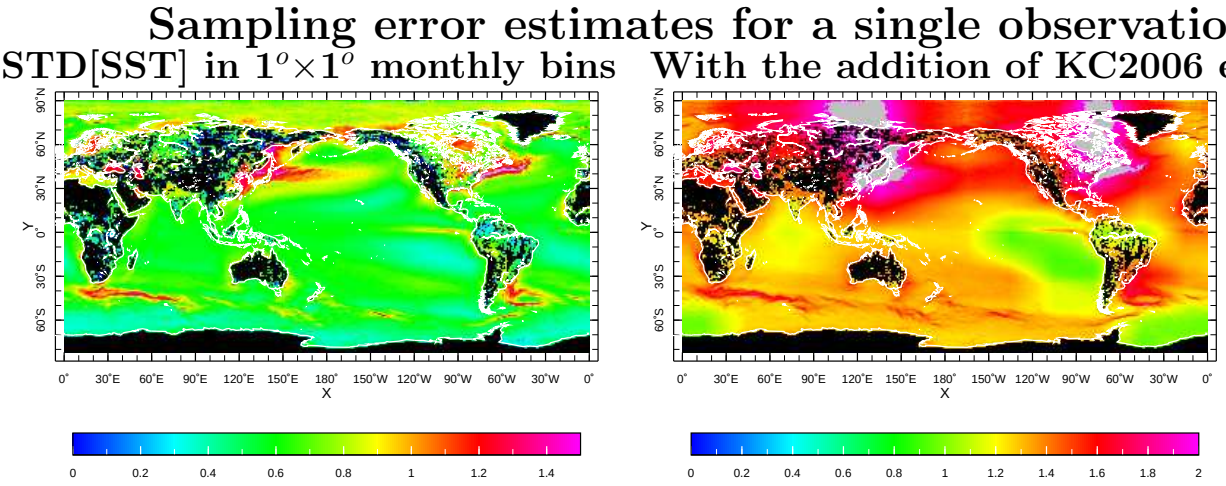

Figure 12: Adding the value of measurement error from *Kent and Challenor* [2006] (KC2006) to the space×time variability in the SST measurements.

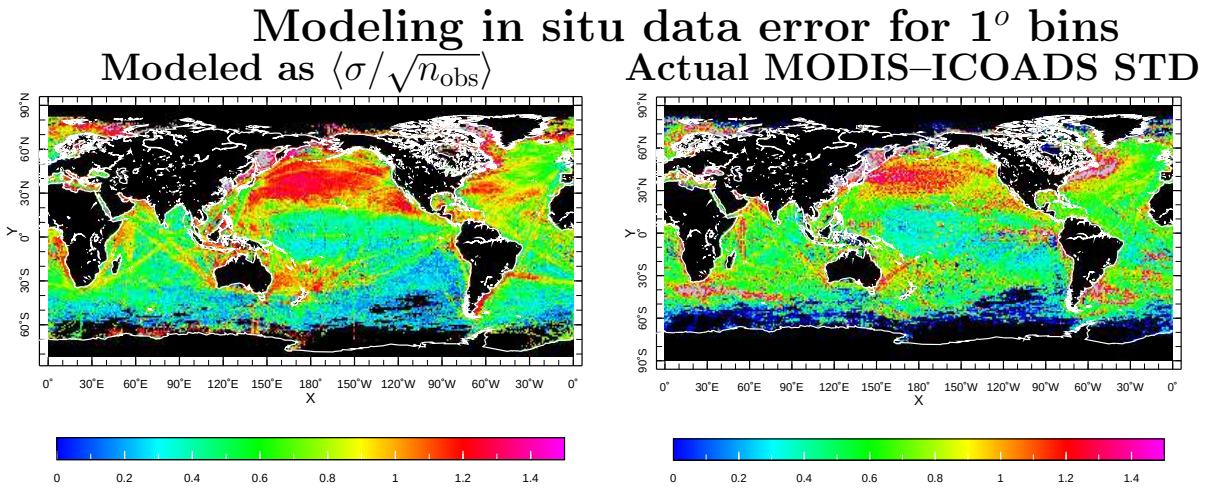

Figure 13: Modeling in situ data error as $\langle \sigma / \sqrt{n_{\rm obs}} \rangle$.

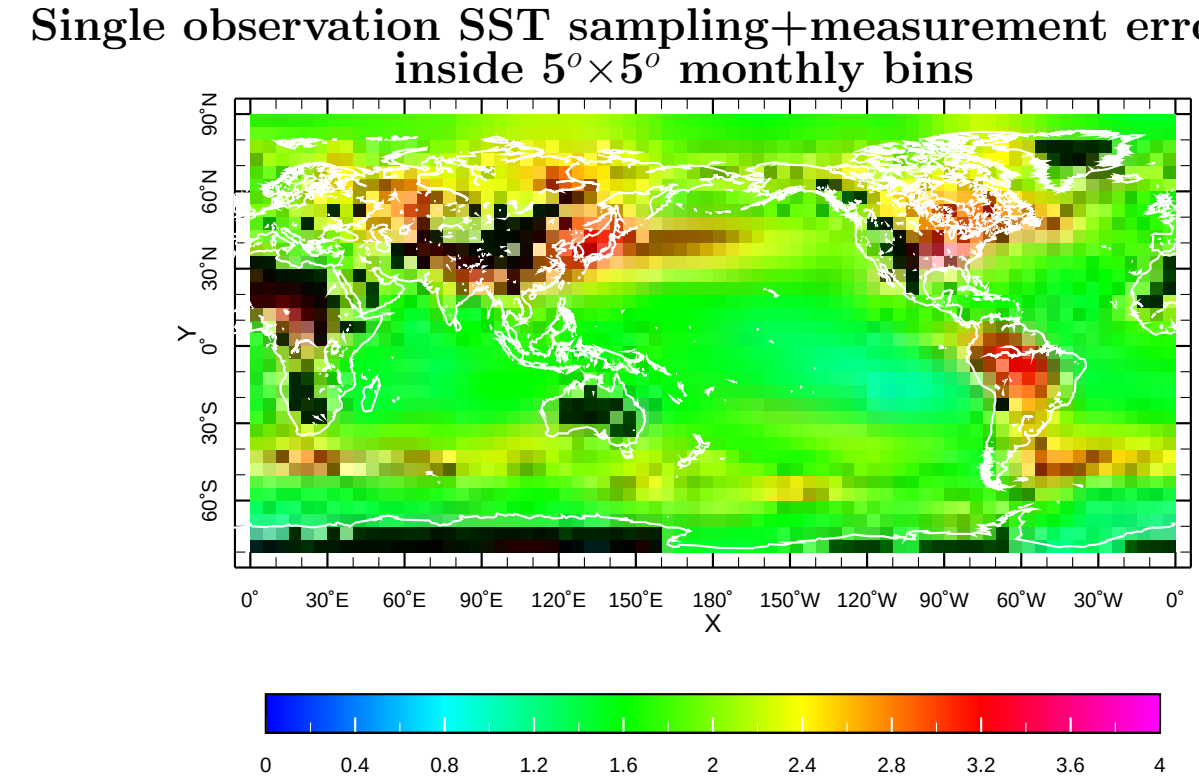

Figure 14: Single observation SST sampling+measurement error, ^{o}C, inside $5^o \times 5^o$ monthly bins

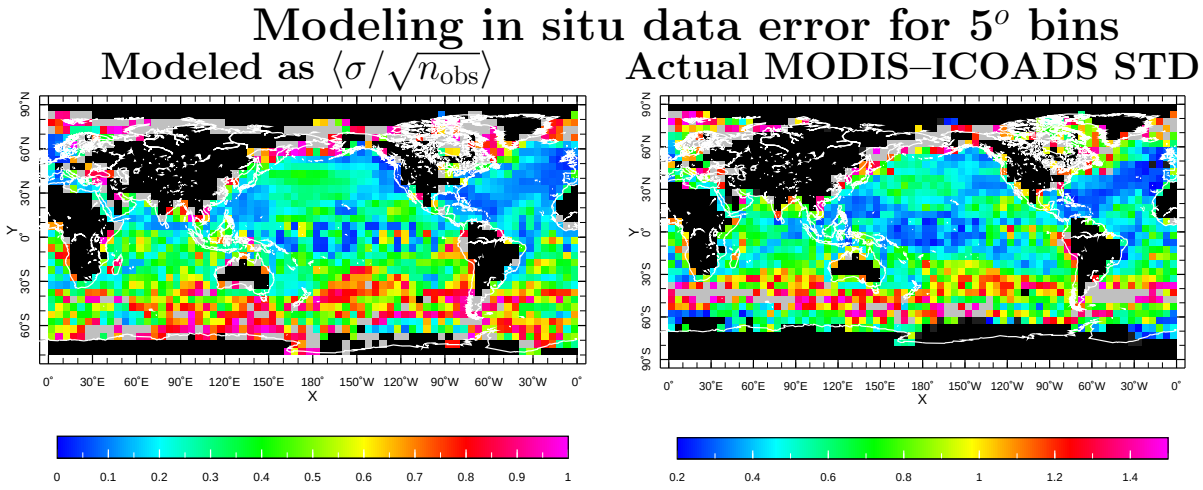

Figure 15: Modeling in situ data error as $\langle \sigma / \sqrt{n_{\rm obs}} \rangle$.